Journal of Power Sources 194 (2009) 610–617

Contents lists available at ScienceDirect

Journal of Power Sources

journal homepage: www.elsevier.com/locate/jpowsour

# Mass spectroscopy for the anode gas layer in a semi-passive DMFC using porous carbon plate Part I: Relationship between the gas composition and the current density

M. Shahbudin Masdar, Takuya Tsujiguchi, Nobuyoshi Nakagawa*

*Department of Chemical and Environmental Engineering, Gunma University, 1-5-1 Tenjin-cho, Kiryu, Gunma 376-8515, Japan*

ARTICLE INFO

*Article history:*
Received 14 April 2009
Received in revised form 14 July 2009
Accepted 14 July 2009
Available online 22 July 2009

*Keywords:*
Passive DMFC
Anode gas layer
Porous carbon plate
Mass spectrometry
Partial pressure of methanol

ABSTRACT

*In situ* mass spectroscopy with a capillary probe was conducted for the anode gas layer of a semi-passive direct methanol fuel cell (DMFC) employing a porous carbon plate (PCP) in order to evaluate the gas composition in contact with the anode. Different types of PCPs were used for the DMFC, and then the relationship between the gas composition in the gas layer and the current density was investigated. The profiles of the $CO_2$ gas pressure, methanol and water vapor pressures were discussed on the basis of the current density and the resistance for the methanol and $CO_2$ transport through the PCP. The current density linearly and identically increased with the increase in the partial pressure of methanol, $P_{CH_3OH}$, in the gas layer up to 7.5 kPa irrespective of the type of the PCP suggesting that the current was a function of $P_{CH_3OH}$ and it was rate limited by the methanol transport to the anode. The calculated liquid methanol concentration equivalent to the measured gas mixture in the gas layer was about 5–7 M in the optimum conditions. This confirmed that the actual methanol activity on the anode of the DMFC with the PCP was controlled by the PCP and was similar to that of the usual liquid feed DMFC even when a very high concentration of methanol was in the reservoir.



## 1. Introduction

The direct methanol fuel cell (DMFC) based on a polymer electrolyte membrane has received much attention as a leading candidate for power source applications because of its high energy density and energy-conversion efficiency [1–5]. However, the commercialization of the DMFC is still hindered by several technological problems [6–8] including methanol crossover (MCO) through the polymer membrane, low electro-catalytic activity of methanol oxidation on the anode [9] and severe cathode flooding [10].

As a result of the MCO, the low concentrations of methanol from 1 to 3 M [11,12,27] under active conditions and about 5 M [13–15,28] under passive conditions have generally shown a maximum performance in the power generation of the DMFC operation. The difference in the optimum concentration between the active and passive conditions must be mainly due to the difference in the mass transfer situation of methanol from the reservoir or flow field to the anode surface, and actual activity of the methanol at the anode surface for the maximum performance would be similar to each other. Actually, by applying a porous carbon plate (PCP) at the anode [16–20], the optimum concentration increased to 16 M or higher, even to 100% methanol, by controlling mass transport of methanol with the PCP. This technique was quite effective to increase the energy density of the DMFC system [19]. In the electrode with PCP, a gas layer with $CO_2$ formed on the anode surface by the accumulation of $CO_2$ gas produced at the anode in a thin empty space between the anode and PCP, and hence, methanol was forced to transport in the vapor phase. A previous paper reported that the gas layer plays an important role in the reduction of MCO and the stabilization of the power generation of the DMFC [17]. Therefore, we understood that the passive DMFC with PCP was substantially operated as a vapor feed DMFC. We have considered that the actual methanol activity on the anode surface of the DMFC with PCP would be similar to that of the conventional DMFC without PCP. However, the gas composition in the gas layer has not yet been measured or confirmed. One of the main objectives of this paper is to measure the gas composition in the gas layer formed on the anode surface of the DMFC with PCP.

For the vapor feed DMFC, a small number of research studies have been reported [21,22,25]. It has the potential for shorter start-up times, because the mass diffusivity is several orders of magnitude greater than that in the liquid phase [23]. However, for high temperature operations, a limitation will arise when using additional equipment such as a heater, pump or vaporizer to vaporize the liquid methanol. The utilization of the additional equipment decreases the system efficiency [24], and it is incompatible with the

* Corresponding author. Tel.: +81 277 30 1458; fax: +81 277 30 1457.
*E-mail addresses:* nakagawa@cee.gunma-u.ac.jp, nakagawa@bce.gunma-u.ac.jp (N. Nakagawa).

0378-7753/$ – see front matter © 2009 Elsevier B.V. All rights reserved.
doi:10.1016/j.jpowsour.2009.07.027

**Table 1**
PCPs properties.

| PCP | Thickness (mm) | Bubble point pressure (kPa) | Average pore diameter (μm) | Darcy constant, $k$ ($m^2$) | Resistance, $R$ ($m^{-1}$) |
|---|---|---|---|---|---|
| Y1 | 1.0 | 7.0 | 1.9 | 4.2E − 14 | 2.4E + 10 |
| Y1.5 | 1.5 | 2.0 | 10.6 | 3.1E − 13 | 4.9E + 09 |
| Y2A | 2.0 | 4.7 | 1.6 | 2.5E − 13 | 8.1E + 09 |
| Y2B | 2.0 | 1.1 | 17.3 | 8.7E − 13 | 2.3E + 09 |

need for passive approaches for a portable DMFC. Recently, a vapor feed DMFC that was passively operated at ambient temperature was reported by some researchers [16–20,26]. However, they did not mention or study the vapor pressure of methanol in the anode chamber. In such a vapor feed DMFC, water management is sometimes critical for the power generation performance [24]. Not only the methanol vapor pressure, but also the water vapor pressure would affect the power generation.

In this study, we investigated the gas composition of the anode gas layer for the DMFC with PCP by *in situ* mass spectrometry. Different conditions of the gas layer were prepared using various methanol concentrations up to 100% and different types of PCPs with different resistance for the methanol transport. The vapor pressure of the gas components, i.e., methanol, water, and other gasses including the reaction products, in the anode gas layer was directly measured by mass spectrometry with a capillary probe. The relationship between the gas condition in the gas layer and DMFC performance was discussed on the basis of the methanol and water vapor pressures, while the formation of the reaction products will be described in the following paper, Part II.

## 2. Experimental

### 2.1. Semi-passive DMFC with a PCP

Four types of PCPs supplied from Mitsubishi Pencil Co. Ltd., were used in the DMFC in this study. The perm-porosimeter (Porous Materials Inc.) was used for the measurement of the properties of PCP, i.e., resistivity to a fluid flow through the PCP and the pore structure like pore diameter. Darcy constant's, $k$ ($=F\mu L/(A\Delta P)$, where, $F$, volumetric flow rate of the fluid; $\mu$, viscosity of the fluid; $L$, thickness of the porous plate; $A$, surface area; $\Delta P$, pressure drop through the plate), for air flow was obtained, and the bubble point pressure was also measured using Galwick solution with surface tension 15.7 dyne $cm^{-1}$ for the different PCP. The analyzed properties for the different PCPs are shown in Table 1. By using these PCPs with different resistances for the methanol transport through it, the gas composition in the anode gas layer was varied, especially for the vapor pressures of methanol and water that would directly affect the DMFC performance. The resistance, $R$ ($=L/k$), shown in the table was calculated based on the Darcy constant, $k$, and the thickness, $L$, and was used as an indicator to show the resistance of the methanol transport through the PCP.

Meanwhile, MEA with a 5 $cm^2$ area, in which Pt and Pt-Ru black were used as the catalyst for the cathode and anode, respectively, was prepared in the same manner as described in our previous papers [16–20]. The catalyst loading was 10 mg $cm^{-2}$ for Pt and 12 mg $cm^{-2}$ for Pt-Ru while Nafion 112 was used as the membrane electrolyte.

The semi-passive DMFC employing PCP used in this study was similar to our previous DMFC [20] and the schematic is shown in Fig. 1. For the gas sampling, we made a slight modification in our previous cell by putting a gas spacer, with a 3.0 mm thickness, between the PCP and the anode current collector. Therefore, the space for the anode gas layer was increased by 3.0 mm when compared to the original cell structure. The capillary probe from the mass spectrometer was inserted through a hole in the spacer and placed in the middle of the space for the gas layer as shown in Fig. 1. The cathode was covered with a thin chamber, and oxygen from a cylinder was flowed through the chamber in order to collect the exhaust gas.

### 2.2. Evaluation of the methanol and water flux

The average methanol flux, i.e., MCO, and water flux through the MEA during the cell operation at a constant cell voltage for the certain time, i.e., the $i$–$t$ measurement for 4 h, were evaluated on the basis of the losses of methanol and water in the reservoir subtracted by the amounts that used for the anode reaction assuming the complete oxidation of methanol to $CO_2$ as follows,

$$CH_3OH + H_2O \rightarrow CO_2 + 6H^+ + 6e^-$$

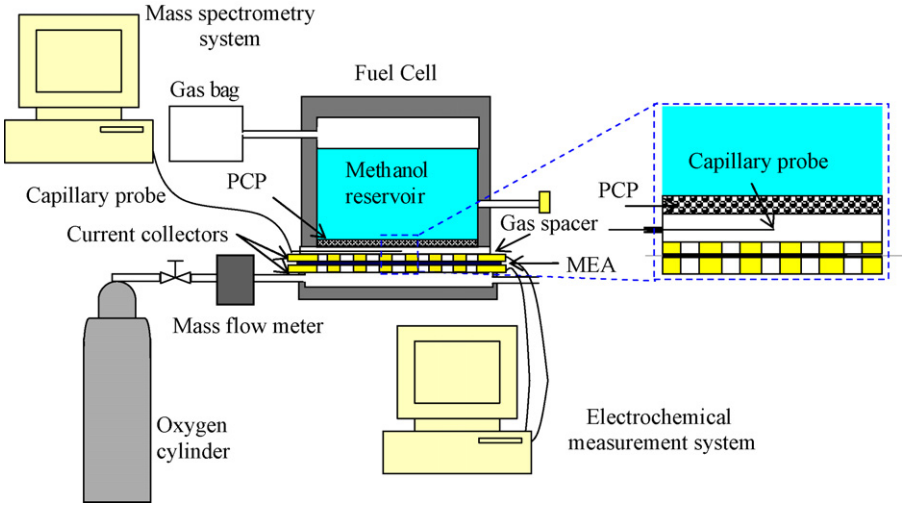


**Fig. 1.** Experimental setup that combined a passive DMFC with PCP and a mass spectrometer.

**Table 2**
Relative abundance intensity of mass spectra results for possible components present in the anode gas layer ($m/z$ = 18–75).

| Mother molecule | Mass per charge ($m/z$) | | | | | | | | | | | | | |
|---|---|---|---|---|---|---|---|---|---|---|---|---|---|---|
| | 18 | 22 | 28 | 29 | 30 | 31 | 32 | 40 | 44 | 45 | 46 | 47 | 60 | 75 |
| Methanol | 0.008 | – | 0.05 | 0.45 | 0.066 | 1.00 | 0.67 | – | – | – | – | – | – | – |
| Water | 1.00 | – | – | – | – | – | – | – | – | – | – | – | – | – |
| Formaldehyde | – | – | 0.23 | 1.00 | 0.58 | 0.00 | 0.00 | – | – | – | – | – | – | – |
| Formic acid | – | – | 0.17 | 1.00 | 0.017 | 0.006 | 0.002 | – | 0.10 | 0.48 | 0.61 | – | – | – |
| Methylformate | 0.01 | – | 0.05 | 0.46 | 0.06 | 1.00 | 0.46 | – | 0.013 | 0.009 | 0.001 | – | 0.38 | – |
| Methylal | 0.001 | – | 0.02 | 0.44 | 0.03 | 0.12 | 0.006 | – | 0.024 | 1.00 | 0.022 | 0.032 | – | 0.44 |
| Carbon dioxide | – | 0.019 | 0.06 | – | – | – | – | – | 1.00 | 0.012 | 0.004 | – | – | – |
| Carbon monoxide | – | – | 1.00 | 0.02 | – | – | – | – | – | – | – | – | – | – |
| Oxygen | – | – | – | – | – | – | 1.00 | – | – | – | – | – | – | – |
| Nitrogen | – | – | 1.00 | 0.01 | – | – | – | – | – | – | – | – | – | – |
| Argon | – | – | – | – | – | – | – | 1.00 | – | – | – | – | – | – |

To do this, a weight loss of the solution in the reservoir was measured, and concentrations of methanol and water in the solution were analyzed before and after the cell operation using a gas chromatography with TCD detector and a Porapack-T column. Then, the charge passed also was calculated by integrating the area of $i$–$t$ curve. The procedure of evaluation of the fluxes was described in detailed in our previous paper [17].

### 2.3. DMFC operation and gas analysis

The experimental setup for the analysis of the gas components during the DMFC operation is shown in Fig. 1. The DMFC with the PCP was operated by injecting a methanol solution with a certain concentration into the reservoir and by feeding oxygen to the cathode at 35 ml min$^{-1}$ under ambient conditions. Power generation was conducted at a certain cell voltage over 4 h. The electrochemical performance of the cell was measured using an HZ3000 electrochemical measurement system (Hokuto Co. Ltd.). The cell temperature was measured at the surface of the cathode by a thermocouple.

For the mass spectral analysis of the gas in the layer, a quadrupole mass spectrometer (DME 100 MS, Ametek Process Instruments) with a capillary probe was used. The mass spectrometer consisted of a quadrupole mass analyzer using a Faraday cup detector with the mass resolution of $m/z$ 0.5 atomic mass units (AMU) at 10% height and a mass range up to 100 AMU. The Faraday cup detector enables partial pressure measurements from $10^{-4}$ mbar to ultrahigh vacuum, $10^{-12}$ mbar. The stability of the mass unit and peak height was high and the error percentage contributions for these stabilities were only ±0.1% and ±2.0%, respectively. The spectrometer utilized an electron impact (EI) ion-

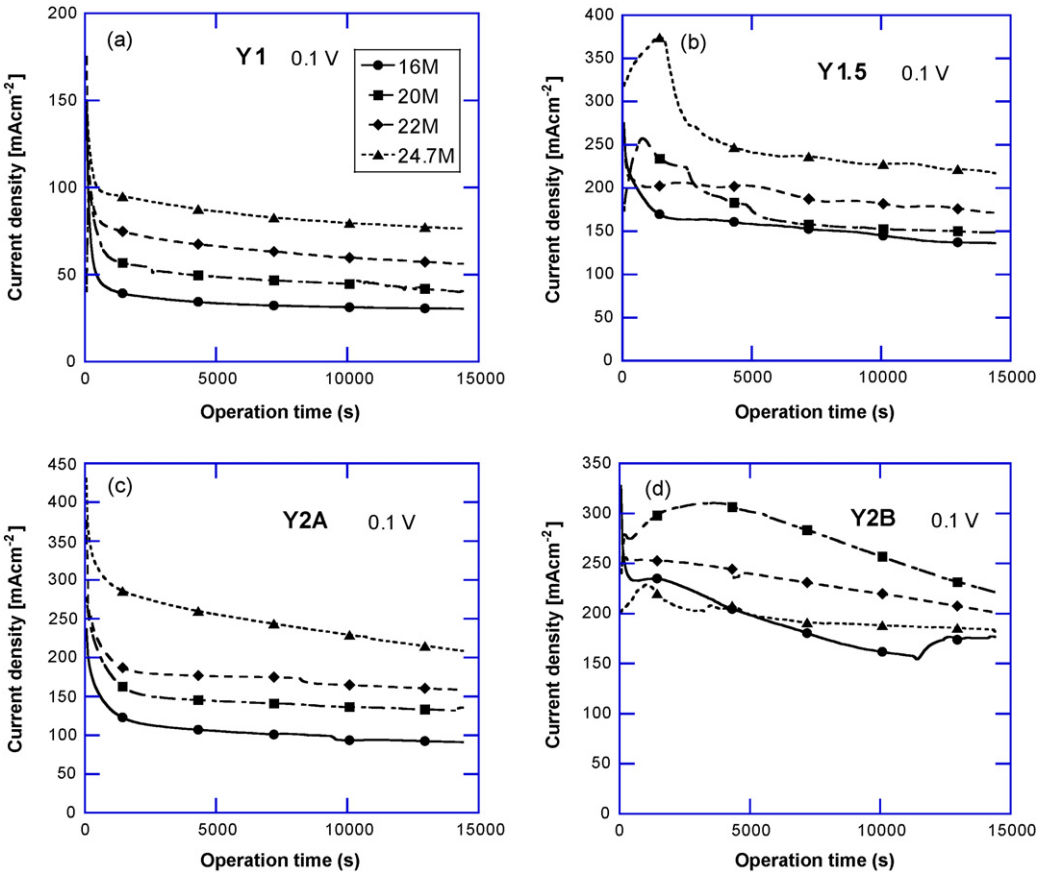


**Fig. 2.** Current density profiles during cell operation at high methanol concentrations and 0.1 V with different types of PCPs (a) Y1, (b) Y1.5, (c) Y2A and (d) Y2B.

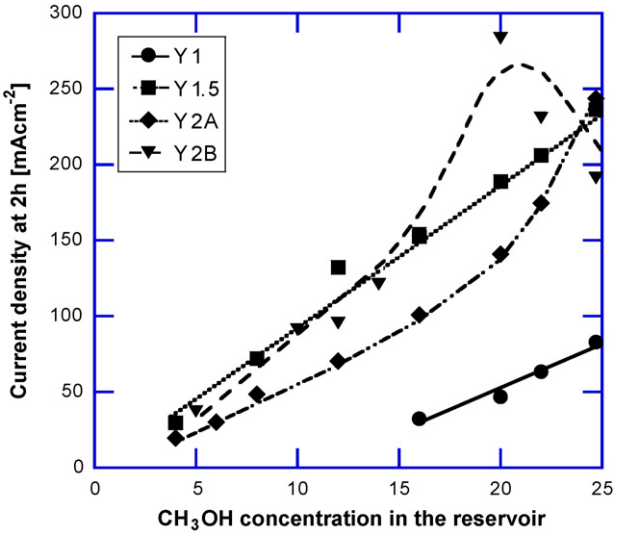


**Fig. 3.** Current density profiles at 2 h steady state condition for different methanol concentrations and different types of PCPs.

ization source and the quadrupole mass spectrometer that was connected to the capillary probe having a 1 m length and 30 μm inner diameters. The capillary probe was placed in the middle of the anode gas layer during cell operation. Data collection was achieved using the fully developed mass spectrometry software DYCOR SYSTEM 2000 and the DYMAXION series DYCOR SYSTEM 2000.

### 2.4. Calibration for the mass spectrometry

The data collection from the mass spectrometer provided the mass spectrum profile (ion current intensity versus mass per charge, $m/z$). The calibration experiments for the conversion of the ion current intensity into vapor pressure was conducted to determine the sensitivity factor for each component by measuring the vapor pressure of the pure component under a certain condition or standard gas of which the composition had been analyzed. For the possible species, such as methanol, water and reaction products including methylformate, formaldehyde and formic acid, the liquid pure component of about 250 ml was placed in a 500 ml bottle which was nearly closed and then immersed in a water bath. The gas atmosphere in the bottle was measured using the capillary probe, and then the sensitivity for the species was obtained on the basis of the vapor pressure calculated under the stated condition. On the other hand, for the gaseous species, such as carbon dioxide, $CO_2$; oxygen, $O_2$ and nitrogen, $N_2$, a calibration was carried out using the standard gas.

The relative abundance data, shown in Table 2, for the possible species in this experiment were taken from the NIST Chemistry WebBook [29] and were used for the quantitative analysis. Although most of these possible species give common mass fragments at $m/z = 1$ for hydrogen, $[H]^+$, $m/z = 12$ for carbon, $[C]^+$ and $m/z = 16$ for oxygen $[O]^+$, we have omitted these fragments in the calculation for a simple treatment, and considered the mass fragments in the range $18 \leq m/z \leq 75$ as shown in the table. The contribution in the ion intensity of each component for a certain mass fragment was separated using the relative abundance data and the ion intensities at different mass fragments. The vapor pressure or partial pressure of each component was then calculated from the contribution in the ion intensity for the main mass fragment of the component using the sensitive factor obtained by the calibration.

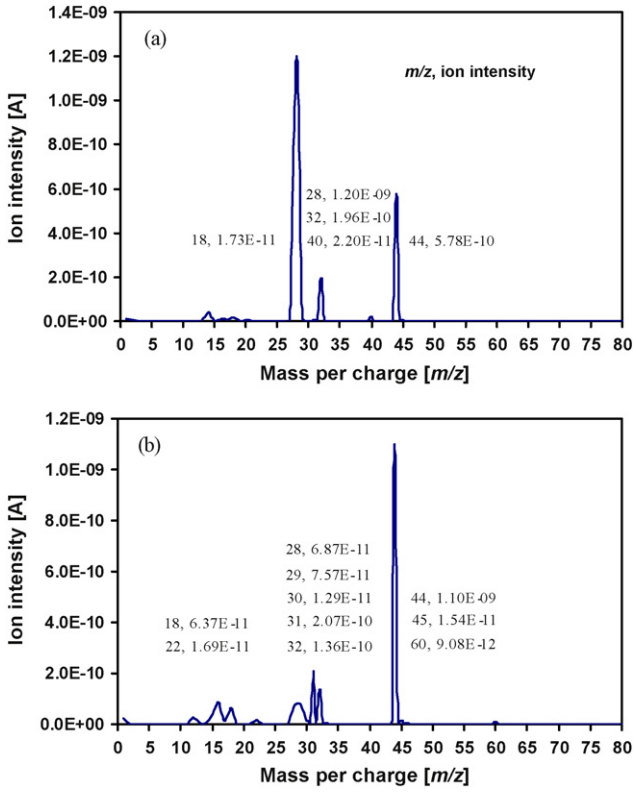


**Fig. 4.** Mass spectrum at 1–80 AMU for the anode gas layer using neat methanol and Y1 for the cell operation at a certain time (a) 2 min and (b) 2 h.

## 3. Results and discussion

### 3.1. Current density profile

Fig. 2 shows the profiles of the current density with time for the DMFC using different PCPs at high methanol concentrations above 16 M. The operation using such high methanol concentrations in the DMFC was enabled with PCP that controls the rate of methanol transport. For all the cases in this figure, at the beginning of cell operation, the current densities showed unstable values with largely decreasing or sometime increasing before became sta-

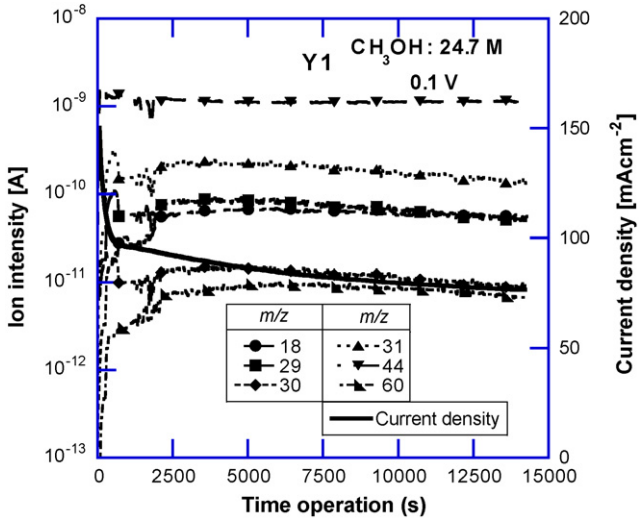


**Fig. 5.** Ion intensity profiles for the main mass per charge for the anode gas layer during cell operation.

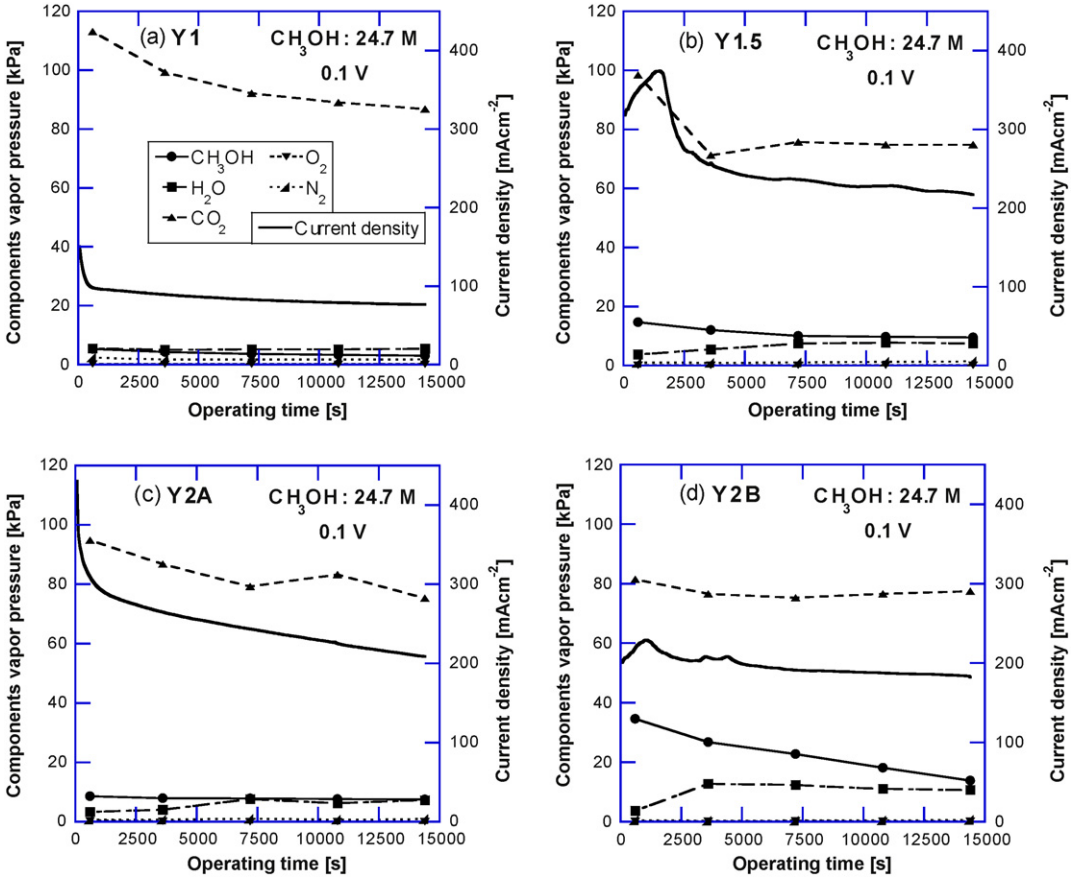


**Fig. 6.** Component species in the gas layer detected by the mass spectrometry during cell operation for neat methanol and different PCP types (a) Y1, (b) Y1.5, (c) Y2A and (d) Y2B.

ble with time. The unstable current density would be related to the initial methanol that accumulated in the PCP under the open circuit conditions and has been explained in our previous reports [18,19]. From the figure, after 7200 s operation, the stable current densities increased with the increasing methanol concentration except the case of using Y2B as shown in Fig. 2 (d). When the stable current densities proportionally increased with increasing current density, the current density must be determined by the rate of methanol transport to the anode, i.e., the rate of methanol transport through the PCP. The current densities at 2 h in the measurement of Fig. 2 were summarized in Fig. 3 including additional data obtained at low methanol concentrations below 16 M.

As clear from Fig. 3, it was a linear dependence of current density on methanol concentration, up to neat in case of Y1, 20 M in case of Y2A and Y1.5 while up to 16 M in case of Y2B. After 20 M, in case of Y2A and Y1.5, there was still a linear dependence of current density on methanol concentration but with different slope up to neat. Meanwhile, in the case of Y2B a large difference of slope until 20 M, then negative slope appeared up to neat.

The linear dependence of current density on the concentration suggested that the cell operation was under the rate controlling by the methanol transport, and the reciprocal of the slope of the line corresponds to the resistance for the methanol transport for the PCP. When the slope of the straight line in Fig. 3 was compared with the resistance, $R$, for the PCP shown in Table 1, one can see a very good correlation between them, suggesting that the methanol transport through the PCP was governed by the Darcy's Law. The steeper the slope the higher the resistance, Y1($R$ = 2.4E + 10 m$^{-1}$) > Y2A (8.1E + 9 m$^{-1}$) > Y1.5 (4.9E + 9 m$^{-1}$) > Y2B (2.3E + 9 m$^{-1}$). For specific PCPs, Y2A and Y2B, the bend of the line means the change of the rate controlling step. We understood that either the electrode reaction or water supply to the anode would be the rate controlling step at higher methanol concentrations instead of the methanol supply. The change of the slope at 16 M for the case of Y2B would be due to high MCO occurred that could not controlled by that PCP. This was because the cell temperature increased, over 5 °C comparing with the cases at lower concentration, at 20 M for the case of Y2B. On the other hand, the negative slope over 20 M would be caused by water deficient at the anode.

### 3.2. Component detected by mass spectrometry

Fig. 4 shows the ion current profiles for the mass fragment, $m/z$, in the range 1–80 AMU in the anode gas layer obtained at 2 min; Fig. 4 (a), and at 2 h; Fig. 4 (b), using Y1. At the beginning of the operation, below 1 min, not shown in the Fig. 4, the air component dominated the anode gas layer. At 2 min, Fig. 4 (a), the peak at $m/z$ = 44, $[CO_2]^+$, for $CO_2$ which is produced by the anode reaction clearly appeared with the main peaks at $m/z$ = 28 for nitrogen, $[N_2]^+$, and at $m/z$ = 32 for oxygen, $[O_2]^+$, in the gas layer as shown in Fig. 4 (a). With time, the vapor pressures of methanol, $m/z$ = 31, $[CH_3O]^+$, and water, $m/z$ = 18, $[H_2O]^+$, increased, while the partial pressures of oxygen and nitrogen decreased by replacing them with $CO_2$ and the methanol as well as the water vapors as shown in Fig. 4 (b). As shown in the figure, the peaks for $m/z$ = 29 and 30 also increased due to the contribution of the relative abundance of methanol as shown in Table 2. Another minor peak was found at $m/z$ = 60, for methylformate, $[HCOOCH_3]^+$, as a minor reaction product. We evaluated not only the major components like $CO_2$, methanol and water, but also the minor products of the methanol oxidation, the behavior of

these minor products are not discussed in this paper. That will be discussed in the following paper, Part II.

As an example of the original profile of the ion current intensity in a logarithmic scale for the real time operation, the profile for the 4 h DMFC operation with Y1 at 24.7 M is shown in Fig. 5. The figure includes the profiles for the several major mass fragments, $m/z$ = 18, 29, 30, 31, 44 and 60, and also the current density obtained from the DMFC. It was confirmed that the $m/z$ = 44, mostly for $CO_2$, always dominated the anode gas layer during the cell operation. The $CO_2$ in the gas layer plays an important role as a barrier to prevent a high MCO through the membrane as mentioned in the previous papers [16–18].

### 3.3. Gas composition in the anode gas layer

Fig. 6 shows the time profiles of the partial pressures for the main components present in the gas layer of the DMFC operated at 100% (24.7 M) methanol in the reservoir. By comparing Fig. 6(a) to (d) for the different PCPs, it was common, among the different PCPs, that the main component was $CO_2$, followed by methanol and water, and the partial pressures of $N_2$, $P_{N2}$, and $O_2$, $P_{O2}$, were negligibly small. It was clear from the figure that the partial pressure of methanol, $P_{CH_3OH}$, and the other components were different from each other depending on the PCP used. This would be related to the difference in the resistance of the PCP for the methanol transport through the PCP as mentioned before. The $P_{CH_3OH}$ at 2 h, at a steady state, was increased from 3.6 kPa for Y1, 7.9 kPa for Y2A, 10.0 kPa for Y1.5, and 22.9 kPa for Y2B. The increasing of $P_{CH_3OH}$ would be related to the decreasing of the PCPs resistance, $R$, in the same order Y1, Y2A, Y1.5 and Y2B, as shown in Fig. 3.

In Fig. 6, the time profile of the current density during the operation was also included. The profile of current density was strongly correlated with $P_{CH_3OH}$ and the partial pressure of $CO_2$, $P_{CO_2}$. This correlation is easily understood because methanol and $CO_2$ are the reactant and the product of the anode reaction, respectively. As cell operated under limiting current, hence, the current density increased with the increasing $P_{CH_3OH}$.

At the beginning of the operation, the initial current density was high due to the sufficient methanol in the PCP, as we mentioned above. Hence, the $P_{CO_2}$ was initially high. For the gas layer formed in the space between the anode and the PCP, the total pressure was determined from the balance between the production rate of $CO_2$ and other gases and the pressure drop for the gas flow out through the PCP. After a few minutes from the start, the current density was controlled by the rate of methanol transport through the PCP, and hence, $P_{CO_2}$ was controlled. The $P_{CO_2}$ at 2 h were 92 kPa for Y1, 81 kPa for Y2A, 78 kPa for Y1.5 and 77 kPa for Y2B. The decreasing of $P_{CO_2}$ in this order would be related to the decreasing of the PCP resistance to the gas flow, i.e., bubble point pressures which were in the same order of decreasing of 7.04 kPa for Y1, 4.65 kPa for Y2A, 2.01 kPa for Y1.5 and 1.10 for Y2B as shown in Table 1.

With respect to water, the vapor pressure, $P_{H_2O}$, gradually increased with time. This would be related to the effect of the back diffusion of water from the cathode to the anode as reported in our previous paper [17]. This phenomenon would gradually increase the $P_{H_2O}$ in the anode gas layer with time. This condition continued until 3600–7200 s before it became nearly constant, i.e., steady state.

Fig. 7 shows the vapor pressure of methanol and water in the DMFC for different PCPs measured at 2 h as a function of the methanol concentration in the reservoir. For all the PCPs, the methanol and water vapor pressures had a tendency to increase with the increasing methanol concentrations in the reservoir. This tendency was varied from one PCP to another depending on its resistance. In the case of $P_{H_2O}$, the increasing value would be related to the water back diffusion. As cell operated under limiting current, the current density increased with increasing methanol concentration thereby water back diffusion would be increased.

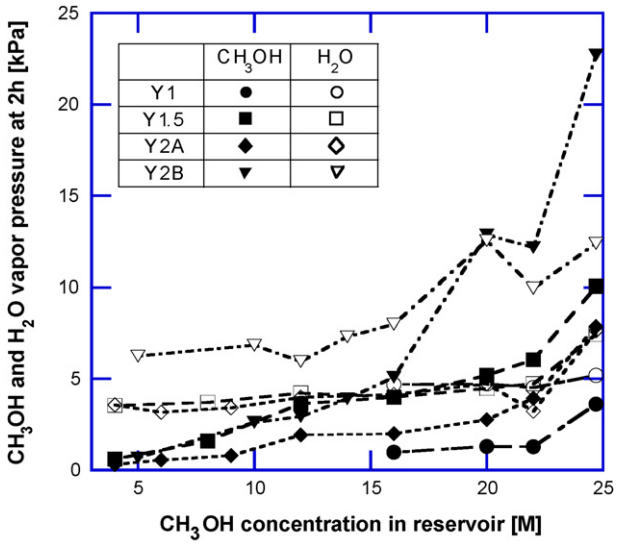


**Fig. 7.** Methanol and water vapor pressure in the anode gas layer using different types of PCPs and methanol concentrations in the reservoir.

### 3.4. Relationship between the current density and the methanol vapor pressure

Fig. 8 shows the relationship between the $P_{CH_3OH}$ in the gas layer and the current density at 2 h. The current densities obtained from the different PCPs were plotted along with the identical line irrespective of the PCP type. The current densities linearly increased with increasing $P_{CH_3OH}$ up to a certain vapor pressure, 7.5 kPa, at which 250 mA cm$^{-2}$ was achieved. The $P_{H_2O}$ measured with $P_{CH_3OH}$ was also plotted in the figure using open symbols for the vertical axis right hand side. We could not see any correlations between $P_{H_2O}$ and the current density or $P_{CH_3OH}$. In the low $P_{CH_3OH}$ region, $P_{CH_3OH} < 7.5$ kPa, the current densities were controlled by the rate of methanol transport through the PCP. This is very clear from the linear dependency of current density on $P_{CH_3OH}$. Otherwise, at a

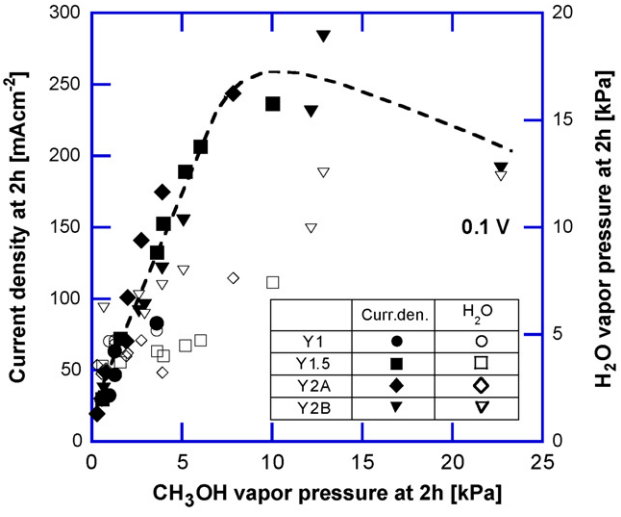


**Fig. 8.** Current density profile and water vapor pressure at various methanol vapor pressures in the gas layer with different PCP types.

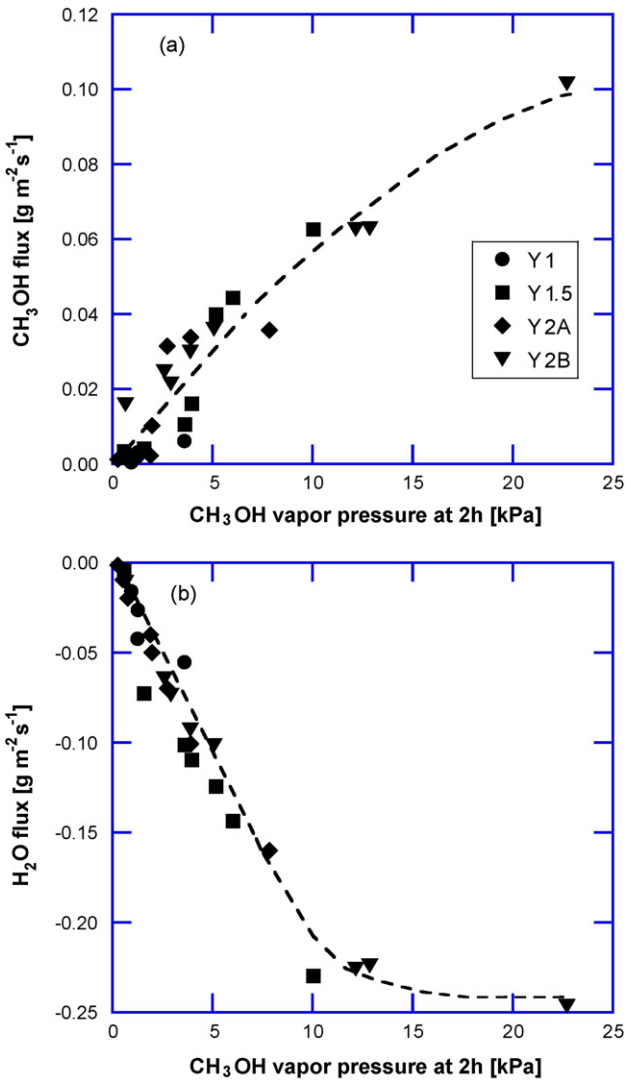


**Fig. 9.** Methanol and water transport through MEA at various methanol vapor pressures in the gas layer with different PCP types (a) Methanol flux and (b) Water flux.

high $P_{CH_3OH}$ above 7.5 kPa, the current density decreased from the maximum current density of 250 mA cm$^{-2}$ with the increasing of $P_{CH_3OH}$. This means that the operation was not under limiting current situation and a high MCO beyond this value occurred.

Fig. 9 shows the relationships among $P_{CH_3OH}$, methanol flux, which corresponds to MCO, and the water flux during cell operation. As shown in Fig. 9 (a), MCO increased with increasing $P_{CH_3OH}$. The value of MCO at $P_{CH_3OH} = 7.5$ kPa, where the change in the rate determining step appeared as shown in Fig. 8, was shown to be about 0.04 g m$^{-2}$ s$^{-1}$. This value of MCO corresponded to the value at which the production rate of methylformate began to increase in a similar passive DMFC used in our previous investigation [26]. This supports the speculation that the rate determining process under limiting current changed at $P_{CH_3OH} = 7.5$ kPa in these experiments. Due to the increase in MCO, the cell temperature increased due to the heat produced by the methanol oxidation at the cathode. The measured cell temperature at the cathode surface was about 40, 45 and 50 °C at 0.04, 0.06 and 0.10 g m$^{-2}$ s$^{-1}$ in MCO, respectively. Meanwhile, the temperature was in the range between 32 and 38 °C at the methanol flux below 0.04 g m$^{-2}$ s$^{-1}$ in this experiment. It was also dependent on the MCO values in that range.

The water flux during the DMFC operation was plotted in Fig. 9 (b). In this study, for all the $P_{CH_3OH}$ values, the water flux was negative indicating that the water back diffusion occurred from the cathode to the anode through the membrane. The water back diffusion linearly increased with the increasing $P_{CH_3OH}$ until 10 kPa where the water flux was −0.22 g m$^{-2}$ s$^{-1}$, and then it became nearly constant in the range $P_{CH_3OH} > 10$ kPa. At the higher $P_{CH_3OH}$, $P_{CH_3OH} > 10$ kPa, it was considered that the water was deficient in the anode reaction.

### 3.4.1. Equivalent liquid methanol concentration

The liquid methanol concentrations that are equivalent for the measured gas compositions, $CO_2$–$CH_3OH$–$H_2O$, for the gas layer were calculated based on the vapor–liquid equilibrium (VLE) assuming an ideal vapor and a non-ideal liquid using the Van Laar model [30]. Table 3 shows the liquid methanol concentrations calculated as equivalent for the gas detected in these experiments. The calculated equivalent liquid methanol concentration obtained in case of 100% methanol in the reservoir was 4.9, 5.5, 4.9, 9.9 M for Y1, Y1.5, Y2A and Y2B, respectively. At the condition where the current density showed the maximum value at 250 mA cm$^{-2}$ for Y2B, the equivalent methanol concentration was calculated to be 7 M. Although the calculated concentration, 7 M, was higher than that of the usual passive DMFC that shows maximum power output at around 5 M, it was reasonable because the point at which the capillary probe set was in the middle of the gas layer, and there was almost a 2 mm distance from the anode surface. The methanol transport in the gas layer would be dominated by gas diffusion. The methanol concentration at the measured point should then show a higher concentration than that of the anode surface. Otherwise, the optimum concentration in the gaseous higher than liquid because MCO occurred in the gas phase is lower than in the liquid phase. Hence, we confirmed that the gas condition in the gas layer of the DMFC with PCP, where the maximum obtained power output was almost equivalent for the liquid methanol concentra-

**Table 3**
Equivalent methanol concentration calculated in the anode gas layer at various methanol concentrations in the reservoir with PCP.

| $CH_3OH$ concentration (M) | Equivalent $CH_3OH$ concentration calculated inside anode gas layer (M) | | | |
|---|---|---|---|---|
| | Y1 | Y1.5 | Y2A | Y2B |
| 4 | – | 0.678 | 0.373 | – |
| 5 | – | – | – | 0.786 |
| 6 | – | – | 0.634 | – |
| 8 | – | 1.618 | – | – |
| 9 | – | 3.350 | 0.866 | – |
| 10 | – | – | – | 2.875 |
| 12 | – | 3.350 | 1.974 | 3.650 |
| 14 | – | – | – | 4.030 |
| 16 | 1.667 | 3.503 | 1.922 | 5.583 |
| 20 | 1.999 | 3.580 | 2.201 | 7.199 |
| 22 | 2.065 | 4.044 | 2.703 | 7.686 |
| 24.7 | 4.905 | 5.545 | 4.949 | 9.895 |

tion at which the usual passive DMFC shows the maximum power output.

## 4. Conclusion

The gas composition in the anode gas layer of the semi-passive DMFC with PCP was directly measured using a mass spectrometer with a capillary probe. As the main components, $CO_2$, methanol and water were detected and the composition was strongly dependent on the PCP used and the methanol concentration in the reservoir. It was shown that $P_{CO_2}$, $P_{CH_3OH}$ and $P_{H_2O}$ were related to the current density and $P_{CH3OH}$ gradually decreased while $P_{H_2O}$ gradually increased with time. The current density linearly and identically increased with the increase in the $P_{CH_3OH}$ in the gas layer up to 7.5 kPa irrespective of the type of PCP used suggesting that the current was rate limited by the methanol transport to the anode. Beyond this value, the current density decreased with the increasing $P_{CH_3OH}$ due to uncontrolled MCO. The calculated liquid methanol concentration equivalent to the $CO_2$–$CH_3OH$–$H_2O$ gas in the gas layer was about 5–7 M in the optimum conditions. This suggested that the actual methanol activity on the anode of the DMFC with PCP was similar to that of the usual liquid feed DMFC even when a very high concentration of methanol was in the reservoir.

## Acknowledgements

A part of this study was supported by JSPS KAKENHI (1936057) and the Nippon Sheet Glass Foundation for Materials Science and Engineering.

## References

[1] B. Kho, I. Oh, S. Hong, H.Y. Ha, Electrochim. Acta 50 (2004) 781–785.
[2] T. Shimizu, T. Momma, M. Mohamedi, T. Osaka, S. Sarangapani, J. Power Sources 137 (2004) 277–283.
[3] D. Kim, E.A. Cho, S.A. Hong, I.H. Oh, H.Y. Ha, J. Power Sources 130 (2004) 172–177.
[4] Q. Ye, T.S. Zhao, J. Power Sources 147 (2005) 196–202.
[5] H. Qiao, M. Kunimatsu, T. Okada, J. Power Sources 139 (2005) 30–34.
[6] S.C. Thomas, X. Ren, S. Gottesfeld, P. Zelenay, Electrochim. Acta 47 (2002) 3741–3748.
[7] Q. Ye, T.S. Zhao, J. Electrochem. Soc. 152 (2005) A2238–A2245.
[8] Z.X. Liang, T.S. Zhao, J. Prabhuram, J. Membr. Sci. 283 (2006) 219–224.
[9] M.Y. Lo, I.H. Liao, C.C. Huang, Int. J. Hydrogen Energy 32 (2007) 731–735.
[10] I. Mizutani, Y. Liu, S. Mitsushima, K. Ota, N. Kamiya, J. Power Sources 156 (2006) 183–189.
[11] S. Surampudi, S.R. Narayanan, E. Vamos, H. Frank, G. Halpert, A.L. Conti, J. Kosek, G.K.S. Prakash, G.A. Olah, J. Power Sources 47 (1994) 377–385.
[12] M.K. Ravikumar, A.K. Shukla, J. Electrochem. Soc. 143 (1996) 2601–2606.
[13] S.R. Yoon, G.H. Hwang, W.I. Cho, I.H. Oh, S.A. Hong, H.Y. Ha, J. Power Sources 106 (2002) 215–223.
[14] R. Chen, T.S. Zhao, J. Power Sources 152 (2005) 122–130.
[15] B. Bae, B.K. Kho, T. Lim, I.H. Oh, S.A. Hong, H.Y. Ha, J. Power Sources 158 (2006) 1256–1261.
[16] N. Nakagawa, M.A. Abdelkareem, K. Sekimoto, J. Power Sources 160 (2006) 105–115.
[17] M.A. Abdelkareem, N. Nakagawa, J. Power Sources 162 (2006) 114–123.
[18] M.A. Abdelkareem, N. Nakagawa, J. Power Sources 165 (2007) 685–691.
[19] M.A. Abdelkareem, N. Morohashi, N. Nakagawa, J. Power Sources 172 (2007) 659–665.
[20] N. Nakagawa, M.A. Abdelkareem, J. Chem. Eng. Japan 40 (2007) 1199–1204.
[21] Z. Guo, A. Faghri, J. Power Sources 167 (2007) 378–390.
[22] H.K. Kim, J. Power Sources 162 (2006) 1232–1235.
[23] J. Rice, A. Faghri, Int. J. Heat Mass Transfer 51 (2008) 948–959.
[24] S. Eccarius, F. Krause, K. Beard, C. Agert, J. Power Sources 182 (2008) 565–579.
[25] I. Chang, S. Ha, J. Kim, J.Y. Lee, S.W. Cha, J. Power Sources 184 (2008) 9–15.
[26] N. Nakagawa, K. Sekimoto, M.S. Masdar, R. Noda, J. Power Sources 186 (2009) 45–51.
[27] J. Ge, H. Liu, J. Power Sources 142 (2005) 56–69.
[28] D. Chu, R. Jiang, Electrochim. Acta 51 (2006) 5829–5835.
[29] http://webbook.nist.gov/chemistry/name-ser.html.
[30] R.H. Perry, in: D.W. Green, J.O. Maloney (Eds.), Perry's Chemical Engineers' Handbook, McGraw Hill, United States, 1997 (pp. 4-1-4-36).